

論文 / 著書情報
Article / Book Information

Title	Surface depletion in doped SrTiO ₃ thin films
Authors	A. Ohtomo, H. Y. Hwang
Citation	Applied Physics Letters, Vol. 84, No. 10,
Pub. date	2004, 3
URL	http://scitation.aip.org/content/aip/journal/apl
Copyright	Copyright (c) 2004 American Institute of Physics

Surface depletion in doped SrTiO₃ thin films

A. Ohtomo^{a)} and H. Y. Hwang^{b)}

Bell Laboratories, Lucent Technologies, Murray Hill, New Jersey 07974

(Received 10 November 2003; accepted 15 January 2004)

Strong effects of surface depletion have been observed in metallic La-doped SrTiO₃ thin films grown on SrTiO₃ substrates by pulsed-laser deposition. The depletion layer grows with decreasing temperature due to the large temperature-dependent dielectric response of SrTiO₃. When the depletion layer becomes comparable to or exceeds the thickness of the doped film, the Hall mobility shows significant enhancements as more of the electron distribution extends into the undoped substrate, in conceptual analogy to modulation doping in compound semiconductor heterostructures. © 2004 American Institute of Physics. [DOI: 10.1063/1.1668329]

Electron-doped SrTiO₃ is a good metal, exhibiting low-temperature Hall mobility in excess of 10 000 cm²/V s.^{1–3} The presence of a nearby ferroelectric instability provides significant screening by polar phonons, resulting in metallic conduction with increasing mobility as temperature decreases, while the electron density remains nearly temperature independent. This is despite a large effective mass estimated at $\sim 10m_0$.¹ Substitutional doping of Nb on the Ti site or La on the Sr site forms hydrogenlike donor states which generate conduction electrons. The semiconductor characteristics of SrTiO₃, as well as the availability of high-quality SrTiO₃ substrates lattice matched to many transition metal oxides, have made thin-film studies of SrTiO₃ central to the notion of “oxide electronics.”

Controlled doping during thin-film growth of SrTiO₃ is complicated by the role of oxygen vacancies, which also generate conduction electrons. This mechanism often dominates below oxygen partial pressures P_{O_2} of 10⁻⁴ Torr in pulsed-laser deposition (PLD).⁴ However, it has also been observed that robust electron doping by Nb substitution during PLD is unsuccessful above a threshold P_{O_2} , which varies depending on the individual growth system.^{5–7} This propensity is suppressed for La-doped films, although the low-temperature carrier mobility is significantly reduced from levels achieved with Nb substitution.⁸ Despite this compromise, many perovskite heterostructures place a premium on well-controlled robust dopant profiles for their function. In this vein, the surface electronic structure of doped and undoped SrTiO₃ has been subject to intensive photoemission studies. Although theoretical studies have predicted a large density of intrinsic surface states,⁹ the effects of surface depletion have not been established in this material,¹⁰ unlike most compound semiconductors.

In this letter, we report the observation of significant surface depletion in metallic La-doped SrTiO₃ thin films. This phenomenon is unusually strong even at high carrier densities, due to the large dielectric background of SrTiO₃,

orders of magnitude higher than in most semiconductors. We estimate a surface pinning potential of ~ 0.7 eV, as deduced from transport measurements and x-ray photoelectron spectroscopy (XPS). For very thin films, we find that the conduction electrons are spatially separated from the doped film and pushed into the substrate by the built-in potential due to surface bandbending, enhancing the low-temperature carrier mobility. Surface depletion is a likely contribution to surface dead layers discussed in many oxide thin films, which are often characterized by large dielectric constants and polar surfaces.

Doped SrTiO₃ films were grown in an ultrahigh-vacuum chamber by PLD, using a single crystal target of La (5 at. %)-doped SrTiO₃. A KrF excimer laser with a repetition rate of 5 Hz was used with fluence at the target surface of ~ 1.7 J/cm², and a target–substrate distance of 45 mm. Buffered HF-etched (001) SrTiO₃ substrates, presenting a TiO₂-terminated surface,¹¹ were used to grow 100–1000 Å films at 800 °C. The thickness was monitored observing unit-cell reflection high-energy electron diffraction (RHEED) oscillations. Molecular O₂ and atomic O, generated by an rf radical source, were used at various partial pressures. After the growth, the temperature was lowered at a constant rate of 50 °C/min, keeping the oxidant gas pressure constant. The transport properties of the films were measured in a conventional Hall bar geometry with ohmic contacts obtained by laser annealing⁴ and Al evaporation. XPS was performed at room temperature for some of the films in a separate analysis chamber.

The basic experimental observation we wish to address can be seen in Fig. 1(a), which shows the temperature-dependent resistivity $\rho(T)$ for a series of films of La_{0.05}Sr_{0.95}TiO₃ with varying thickness, grown in 0.1 Torr of O₂. At these high oxygen pressures, oxygen vacancies in the film are suppressed. With decreasing thickness, ρ increases dramatically, roughly by an order of magnitude going from 1000 Å to 100 Å. The Hall coefficient R_H for the films was measured between 2 K and 300 K, using the film thickness d determined from RHEED oscillations. The Hall effect was linear in magnetic field up to 14 T, and showed no additional structure for all temperatures. The temperature-dependence of the effective three-dimensional carrier density n is given in Fig. 1(b), where $n = -1/(eR_H)$ and e is the electron

^{a)}Present address: Institute for Materials Research, Tohoku University, Sendai, 980-8577, Japan.

^{b)}Also at: Department of Advanced Materials Science, University of Tokyo, Kashiwa, Chiba 277-8561, Japan, and Japan Science and Technology Agency, Kawaguchi, 332-0012, Japan; electronic mail: hyhwang@k.u-tokyo.ac.jp

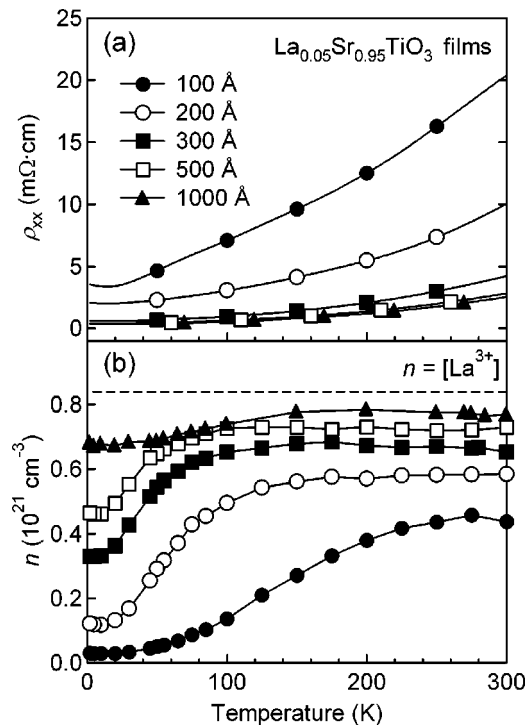


FIG. 1. (a) Temperature dependence of the resistivity ρ for $\text{La}_{0.05}\text{Sr}_{0.95}\text{TiO}_3$ films with varying thickness d ranging from 100 Å to 1000 Å. (b) Temperature dependence of the carrier density n , as deduced from the Hall effect, for the films in (a). The dashed line denotes the ideal carrier density, assuming full activation of the La dopants.

charge, which has been found to be an accurate description in bulk $(\text{La,Sr})\text{TiO}_3$ in this doping range.¹² With decreasing temperature, the carrier densities of all of the films decrease markedly, in contrast to the nearly temperature independent n observed in doped bulk single crystals. However, the loss of carriers is inconsistent with freeze-out, following rather a power law temperature dependence and saturating at a finite value. It is also noteworthy that thinner films show smaller n at all temperatures.

A common interpretation of Fig. 1 is the existence of an insulating dead layer. To consider this issue, we first note that there was no evidence of diminished crystallinity near the surface, from either RHEED or x-ray diffraction. Therefore, we focus on the loss of carriers at the surface over a constant thickness. Figure 2(a) shows d as a function of nd for the films in Fig. 1, which shows linear behavior. The positive vertical intercept gives a measure of the insulating layer thickness d_0 , evaluated as 53 Å at 300 K and 165 Å at 2 K. A similar analysis at all points gives the temperature dependence of d_0 [Fig. 2(b)], which grows significantly with decreasing temperature.

The temperature dependence of d_0 can be understood by considering the expression for a depletion layer

$$d_0 = (2\epsilon(T)\epsilon_0 V_B / en)^{0.5}, \quad (1)$$

where ϵ and ϵ_0 are the SrTiO_3 and vacuum dielectric constants, respectively, and V_B is surface pinning potential. Using $n = [\text{La}^{3+}]$ (asymptotically approached with increasing film thickness and temperature), and a typical value for the dielectric constant of thin-film SrTiO_3 $\epsilon(300\text{ K}) = 300$,¹³ one obtains $V_B = 0.7$ eV to reproduce the observed d_0 at room temperature. Taking the value of $V_B = 0.7$ eV and n as con-

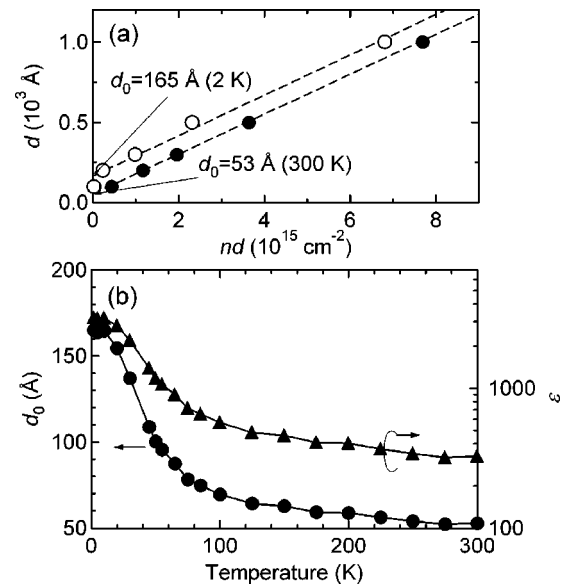


FIG. 2. (a) The relation between film thickness d and nd , for various thickness films. The vertical intercept corresponds to the thickness of the surface insulating layer d_0 , which is evaluated as 165 Å and 53 Å at 2 K and 300 K, respectively. (b) Temperature dependence of the insulating layer thickness d_0 . Also shown is the temperature dependence of the dielectric constant ϵ , as determined from the depletion layer thickness, assuming a surface pinning potential V_B of 0.7 eV and full dopant activation for all temperatures.

stant (consistent with bulk and thick film measurements), $\epsilon(T)$ can be estimated from $d_0(T)$, as shown in Fig. 2(b). The temperature dependence of ϵ is quite similar to that measured in films,¹³ rising by an order of magnitude at low temperatures, but significantly suppressed when compared to bulk single crystals.¹⁴ Therefore, we conclude that the intrinsic carrier density in the films is temperature independent, but the temperature dependence of the depletion layer reduces the total carrier number.

As an independent measure of surface depletion, *ex situ* XPS was performed for several $\text{La}_{0.05}\text{Sr}_{0.95}\text{TiO}_3$ films and a bare SrTiO_3 substrate. Figure 3(a) shows spectra near the valence-band maximum E_V for three films of constant thickness (1500 Å) grown in 1×10^{-6} Torr of O_2 (A), 1×10^{-5} Torr of O (B), and 0.1 Torr of O_2 (C). The carrier density of each film was measured as 8×10^{21} , 1×10^{21} , and 8×10^{20} cm^{-3} , respectively, and all showed metallic conductivity down to low temperature. Films A and B, containing oxygen vacancies, have carrier densities higher than the La^{3+} concentration (8.4×10^{20} cm^{-3}). Considering first the SrTiO_3 substrate, the valence-band edge is consistent with the chemical potential μ fixed close the conduction band by residual impurities and oxygen vacancies. Film C, grown in conditions identical to those in Figs. 1 and 2, shows a decrease in $|E_V - \mu|$, opposite to what would be expected from a Burstein shift. A similar trend is also observed in the shift of the peak positions. With increasing carriers (films B and A), $|E_V - \mu|$ systematically increases, consistent with degenerate semiconductor statistics and conduction-band filling, leading to a typical Burstein shift with respect to film C.

These systematic trends support the picture of bandbending at the surface deduced from transport measurements, since the XPS probing depth (< 20 Å) is shorter than the depletion layer thickness (d_0). Figure 3(b) shows a sche-

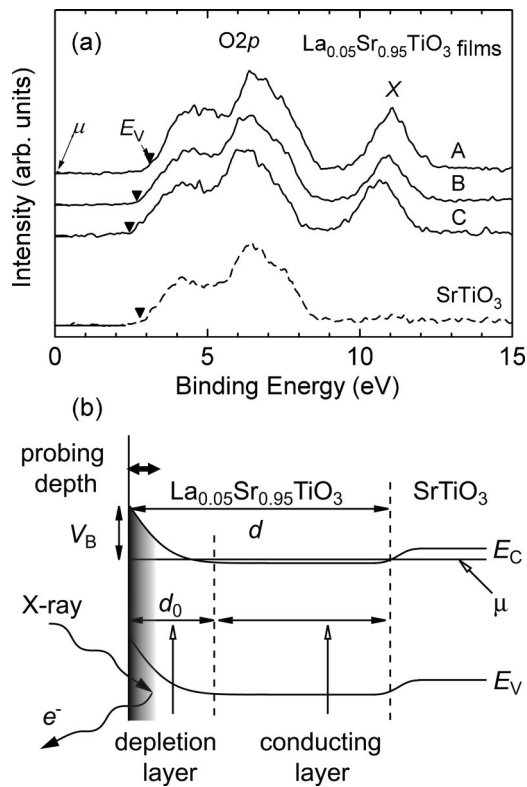


FIG. 3. (a) XPS spectra near the valence-band maximum E_V for 1500 Å thick $\text{La}_{0.05}\text{Sr}_{0.95}\text{TiO}_3$ films and (001) SrTiO_3 single crystal. The films were grown in different conditions: 1×10^{-6} Torr of O_2 (A), 1×10^{-5} Torr of O (B), and 0.1 Torr of O_2 (C). (b) Schematic band diagram of $\text{La}_{0.05}\text{Sr}_{0.95}\text{TiO}_3$ film grown on SrTiO_3 substrate. The depletion layer d_0 is generally thicker than the XPS probing depth (~ 20 Å).

matic energy diagram of the $\text{La}_{0.05}\text{Sr}_{0.95}\text{TiO}_3$ film. The surface pinning potential can be estimated as $V_B = E_g - |E_V - \mu|$, where E_g is room-temperature bandgap of SrTiO_3 , giving $V_B \sim 0.69$ eV, in reasonable agreement to V_B obtained previously. A quantitative analysis of the trend from films C to A is difficult, as the dielectric response of the film may evolve, and the depletion layer at high carrier densities (~ 17 Å in film A) becomes comparable to the electron escape depth. Nevertheless, our results are similar to observations in vacuum-fractured surfaces of $\text{La}_{0.05}\text{Sr}_{0.95}\text{TiO}_3$ single crystals upon oxygen exposure.¹⁵ Positively charged surface defects can attract oxygen and bind free electrons in the bulk, resulting in Fermi-level shifts at the surface. The origin of peak X located around 11 eV in Fig. 3(a), which is not seen for the stoichiometric SrTiO_3 single crystal, is suggested to be the oxygen defect at the surface.^{16,17}

Having established the band diagram of Fig. 3(b) as a reasonable description of our films, we turn now to discuss the temperature-dependent Hall mobility $\mu_H(T)$, shown in Fig. 4. These results are comparable to that of bulk single crystal with identical composition. Although the thinnest 100 Å film should be completely depleted below ~ 50 K [Fig. 2(b)], it is still conducting at 2 K, with twice the low-temperature mobility of the other films. The inset to Fig. 4 shows μ_H at various temperatures as a function of $d - d_0$, the undepleted film thickness. As this value crosses the origin, μ_H is abruptly enhanced. In this configuration, the doped electrons are spatially separated from the La^{3+} donor

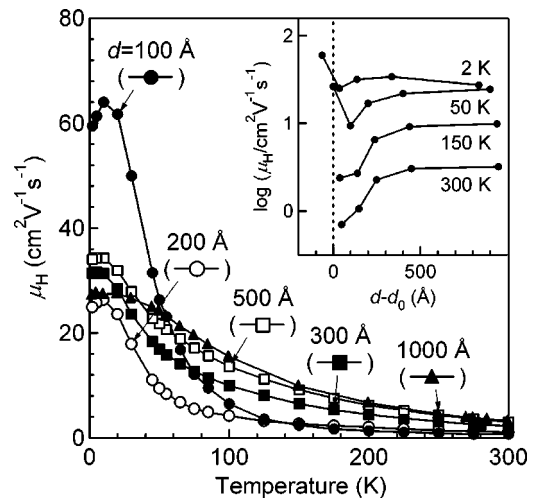


FIG. 4. Temperature dependence of the Hall mobility μ_H for the films shown in Figs. 1 and 2. The inset shows $\log \mu_H$ as a function of $d - d_0$, the undepleted film thickness, at various temperatures. Note that the highest mobility values are seen at negative $(d - d_0)$ in the $d = 100$ Å film at low temperature, corresponding to complete depletion of the doped film.

sites, and distribute into the substrate by the built-in potential arising from surface bandbending. The mobility enhancement arises from this separation, as the conduction electrons are less sensitive to scattering by the ionized La^{3+} impurities. This effect is significant despite the decrease in mobility due to a growing contribution of diffuse surface scattering with decreasing film thickness. Although La -doped SrTiO_3 exhibits relatively low mobility, these results demonstrate, in principle, that the notion of offset doping¹⁸ can be applied to oxide heterostructures as a means of increasing carrier mobilities.

The authors thank R. L. Opila for assistance regarding XPS, and T. Susaki for discussions.

- ¹H. P. R. Frederikse, W. R. Thurber, and W. R. Hosler, *Phys. Rev.* **134**, A442 (1964).
- ²O. N. Tufté and P. W. Chapman, *Phys. Rev.* **155**, 796 (1967).
- ³C. Lee, J. Yahia, and J. L. Brebner, *Phys. Rev. B* **3**, 2525 (1971).
- ⁴A. Ohtomo and H. Y. Hwang (unpublished).
- ⁵K. L. Myers, Ph.D. thesis, Stanford University, 1993.
- ⁶T. Tomio, H. Miki, H. Tabata, T. Kawai, and S. Kawai, *J. Appl. Phys.* **76**, 5886 (1994).
- ⁷A. Leitner, C. T. Rogers, J. C. Price, D. A. Rudman, and D. R. Herman, *Appl. Phys. Lett.* **72**, 3065 (1998).
- ⁸D. Olaya, F. Pan, C. T. Rogers, and J. C. Price, *Appl. Phys. Lett.* **80**, 2928 (2002).
- ⁹T. Wolfram, E. A. Kraut, and F. J. Morin, *Phys. Rev. B* **7**, 1677 (1973).
- ¹⁰R. A. Powell and W. E. Spicer, *Phys. Rev. B* **13**, 2601 (1976).
- ¹¹M. Kawasaki, K. Takahashi, T. Maeda, R. Tsuchiya, M. Shinohara, O. Ishiyama, T. Yonezawa, M. Yoshimoto, and H. Koinuma, *Science* **266**, 1540 (1994).
- ¹²Y. Tokura, Y. Taguchi, Y. Okada, Y. Fujishima, T. Arima, K. Kumagai, and Y. Iye, *Phys. Rev. Lett.* **70**, 2126 (1993).
- ¹³H. C. Li, W. Si, A. D. West, and X. X. Xi, *Appl. Phys. Lett.* **73**, 464 (1998).
- ¹⁴T. Sakudo and H. Unoki, *Phys. Rev. Lett.* **26**, 851 (1971).
- ¹⁵Y. Aiura, I. Hase, H. Bando, T. Yasue, T. Saitoh, and D. S. Dessau, *Surf. Sci.* **515**, 61 (2002).
- ¹⁶B. Reihl, J. G. Bednorz, K. A. Müller, Y. Jugnet, G. Landgren, and J. F. Morar, *Phys. Rev. B* **30**, 803 (1984).
- ¹⁷T. Higuchi, T. Tsukamoto, N. Sata, M. Ishigame, Y. Tezuka, and S. Shin, *Phys. Rev. B* **57**, 6978 (1998).
- ¹⁸R. Dingle, H. L. Stormer, A. C. Gossard, and W. Wiegmann, *Appl. Phys. Lett.* **33**, 665 (1978).